Wild-type KRAS inhibits the migration and invasion of pancreatic cancer through the Wnt/β-catenin pathway

XIANHUA HU[1], RENDAN ZHANG[2], JIAXIN YAO[2], BO MU[2] and CHUNYAN ZHAO[3]

[1]Department of Medical Laboratory; [2]School of Basic Medicine and Forensic Medicine; [3]Sichuan Key Laboratory of Medical Imaging, Institute of Medical Imaging, North Sichuan Medical College, Nanchong, Sichuan 637000, P.R. China

Received August 5, 2022; Accepted October 10, 2022

DOI: 10.3892/mmr.2022.12891

Abstract. Kirsten rat sarcoma virus (KRAS) mutation is considered to be the event that leads to the initiation of pancreatic ductal adenocarcinoma (PDAC), the mutation frequency of the KRAS gene in PDAC is 90-95%. Studies have shown that wild-type KRAS ($KRAS^{WT}$) has a survival advantage in PDAC and can antagonize the effect of mutated KRAS G12D ($KRAS^{G12D}$), leading to a low cell transformation efficiency. The present study focused on the differences in biological behavior between $KRAS^{WT}$ and $KRAS^{G12D}$ and explored the mechanism in pancreatic cancer. Overexpressed $KRAS^{WT}$ and $KRAS^{G12D}$ was transfected into cells through lentiviral transfection. The differences and mechanisms were explored using cell counting kit-8 (CCK-8), clone formation, wound healing and Transwell assays, as well as western blotting, immunohistochemistry and tumor formation in nude mice. *In vitro*, the proliferation of $KRAS^{WT}$ group was reduced compared with PANC-1 group, while the proliferation of $KRAS^{G12D}$ group was not significantly changed. *In vivo*, the proliferation of $KRAS^{WT}$ group was reduced and that of $KRAS^{G12D}$ group was enhanced compared with that in the PANC-1 group. The invasion and migration of $KRAS^{WT}$ group were decreased, while the invasion and migration of $KRAS^{G12D}$ group were increased. Western blotting showed that the expression of E-cadherin, α-E-catenin, MMP-3, MMP-9, STAT3 and phosphorylated STAT3 in $KRAS^{WT}$ group was increased, while no significant difference was observed in $KRAS^{G12D}$ group. The results of immunohistochemistry were consistent with those of western blotting. $KRAS^{WT}$ group can inhibit the proliferation of pancreatic cancer *in vitro* and *in vivo*, while $KRAS^{G12D}$ group can significantly promote proliferation *in vivo*, but not significantly *in vitro*. Wild-type KRAS may inhibit the invasion and migration of pancreatic cancer through the Wnt/β-catenin pathway.

Correspondence to: Ms. Chunyan Zhao, Sichuan Key Laboratory of Medical Imaging, Institute of Medical Imaging, North Sichuan Medical College, 234 Fujiang Road, Nanchong, Sichuan 637000, P.R. China
E-mail: 13699665433@163.com

Key words: pancreatic cancer, wild-type Kirsten rat sarcoma virus, mutant Kirsten rat sarcoma virus, Wnt/β-catenin

Introduction

Pancreatic ductal adenocarcinoma (PDAC) is one of the most malignant tumors of the digestive system. Due to its deep anatomical location and occult clinical manifestations, there are no effective methods for early diagnosis, resulting in a high mortality rate (1). Despite advances in the diagnosis and treatment of pancreatic cancer, with a 5-year survival rate of 9%, PDAC is predicted to become the second leading cause of cancer-related mortality worldwide by 2030 (2).

KRAS mutations are considered to initiate PDAC and the frequency of KRAS mutations in PDAC ranges from 90-95% (3). The dominance of KRAS mutations suggests that targeted therapy against the Ras signaling network may be an effective treatment modality for PDAC. To date, several targeted therapies for PDAC have been approved (4). The first approved was EGFR inhibitor erlotinib, which in combination with gemcitabine had a survival benefit compared to gemcitabine alone, but was effectively abandoned by the community after negative data emerged on EGFR-targeted therapy for KRAS mutant colorectal cancer (5). Then, the TRK kinase inhibitors larotrectinib and entrectinib were approved for solid tumors containing the NTRK-fusion gene. However, the NTRK-fusion gene occurs in only 0.5% of PDAC and the majority of PDAC without the NTRK-fusion gene has not been systematically evaluated (6). Finally, the PARP inhibitor olaparib can extend progression free survival but not overall survival in patients of late-stage PDAC with germline mutations in BRCA1 or BRCA2 (~7.5%) (7). In conclusion, their clinical activity has been disappointing so far. Therefore, there is an urgent need to identify new therapeutic modalities for pancreatic cancer.

It is well known that the vast majority of mutations in Ras are missense mutations in three hotspot residues, G12, G13 and Q61. The order of frequency observed at the G12 is G12D, G12V, G12C, G12A, G12S and G12R and G12C mutation prevalent in lung cancer and G12D being the most common in PDAC. In fact, KRAS G12D ($KRAS^{G12D}$) is one of the most important tumor therapeutic targets (8).

A previous study demonstrated that wild-type KRAS ($KRAS^{WT}$) has a survival advantage in PDAC and patients

with $KRAS^{WT}$ have a longer overall survival time (9). Patients with mutated KRAS have been shown to have worse survival and a shorter overall survival following gemcitabine-based first-line chemotherapy, regardless of age, sex, tumor stage, tumor morphology, or chemotherapy regimen. $KRAS^{WT}$ can antagonize the effects of mutated $KRAS^{G12D}$, resulting in inefficient cellular transformation (10). In addition, the increased dose of mutated $KRAS^{G12D}$ is accompanied by the deletion of $KRAS^{WT}$ in PDAC (11). This suggests that $KRAS^{WT}$ may exert a potential tumor suppressive effect through certain pathways, but the mechanism has not yet been elucidated.

In view of the characteristics of KRAS wild-type and mutant genes in cancer, the present study overexpressed these two genes. It focused on the differences in biological behavior between $KRAS^{WT}$ and $KRAS^{G12D}$ and explored the pathway and mechanism in pancreatic cancer and provides theoretical basis for the study of the KRAS gene.

Materials and methods

Cells and lentiviruses. A PANC-1 human pancreatic ductal adenocarcinoma cell line was provided by the Sichuan Institute of Medical Imaging, the lentivirus was purchased from Shanghai GeneChem Co., Ltd., and $KRAS^{WT}$ and $KRAS^{G12D}$ cells were constructed by the authors.

Lentiviral infection. Lentiviruses expressing $KRAS^{WT}$ and $KRAS^{G12D}$ were generated and purchased from Shanghai GeneChem Co., Ltd. Lentiviruses were infected into cells at a multiplicity of infection (MOI) of 200 for $KRAS^{G12D}$ and 50 for $KRAS^{WT}$. Briefly, cell suspensions of 3-5x10^4/ml were prepared in 96-well plates (100 μl per well) and culture was performed for 18-24 h. According to cell MOI and virus titer, $KRAS^{WT}$ and $KRAS^{G12D}$-overexpressing viruses were added to the wells. Culture was performed at 37˚C for 12-16 h, after which the medium was replaced with conventional medium. Additional culture was performed for a further 3-4 days and the infection efficiency was observed in >10 fields of view under a fluorescence microscope (magnification, x20; Leica DMIL LED; Leica Microsystems, Inc.). The medium was then replaced with medium containing 2 μg/ml purinomycin for further culture (37˚C, 5% CO_2) for over a week and follow-up experiments were carried out.

Cell culture. Cells were cultured in DMEM (Hyclone; Cytiva) containing 10% fetal bovine serum(Gibco; Thermo Fisher Scientific, Inc.), 100 U/ml penicillin, 100 μg/ml streptomycin in a humidified incubator at 37.5˚C with 5% CO_2. Trypsin (0.25%) was used for digestion and subculture at a rate of 1:3. $KRAS^{WT}$ and $KRAS^{G12D}$ cells were cultured and subcultured with DMEM containing 2 μg/ml purinomycin, which was replaced with conventional DMEM during the subsequent experiments.

Reverse transcription-quantitative (RT-q) PCR. The expression of the KRAS gene in transfected KRASWT and KRASG12D cells was detected using RT-qPCR. When cell density was ~80%, total RNA was extracted by TRIzol® (cat. no. 15596026; Invitrogen; Thermo Fisher Scientific, Inc.), cDNA was synthesized (RevertAid First Strand cDNA Synthesis Kit; cat. no. K1622; Thermo Fisher Scientific, Inc.) according to the manufacturer's protocol and qPCR (Power Up™ SYBR™ Green; cat. no. A25742; Applied Biosystems; Thermo Fisher Scientific, Inc.) was performed. All steps were carried out according to the manufacturers' protocols. qPCR was conducted using the Light Cycler 96 (Roche Diagnostics) under the following conditions: 2 min at 50˚C, 2 min at 95˚C, followed by 40 cycles at 95˚C for 15 sec, 57˚C for 15 sec and 72˚C for 1 min. Fold change in expression was calculated using the standard 2-ΔΔCq formula (12). GAPDH was used as an internal loading control and the experiment was repeated three times. The primer sequences were as follows, GAPDH: 5'-ACTAGG CGCTCACTGTTCTCT-3' forward and 5'-GGAATTTGCCAT GGGTGGAA-3' reverse; KRASWT: 5'-GCCTGCTGAAAA TGACTGA-3' forward and 5'-CTCCTCTTGACCTGCTGT G-3' reverse; KRASG12D: 5'-ACACAAAACAGGCTCAGG A-3' forward and 5'-GTCGGATCTCTCTCACCAA-3' reverse.

CCK-8 assay. Cell suspensions of 2x10^4/ml were prepared in 96-well plates (100 μl per well) and five repeats in each group were detected at 24, 48, 72, 96 and 120 h, respectively. CCK-8 reagent (10 μl) was added to each well and incubated at 37˚C for 1 h. Absorbance was then determined at 450 nm by SpectraMax Paradigm microplate reader (Molecular Devices. Inc.).

Colony formation assay. A total of 200 cells/well were inoculated in a 6-well plate and cultured at 37˚C with 5% CO_2 for 2 weeks. When there were visible colonies (>50 cells), cells were washed twice with PBS, fixed with 4% paraformaldehyde for 15 min at room temperature and stained with 0.1% crystal violet for 15 min at room temperature. The dying solution was washed with clear water and dried naturally. The colonies were scanned and their number was counted.

Wound healing assay. Cell suspensions of 1x10^5/well were prepared in a 6-well plate and cultured in a medium containing 10% FBS. The cells were scratched when the monolayer fusion was ~90%. Horizontal lines were drawn at the 6-well plate, cells were washed with PBS and then a position selected where the scratches were clear, followed by further culture with serum-free medium (37˚C, 5% CO_2). Images of the same positions were captured at 0, 24, 48, 72, 96 and 120 h respectively.

Transwell assay. Cell suspensions of 2x10^5/ml were prepared in serum-free medium. A total of 500 μl medium with 10% FBS was added to the lower Transwell chamber and 100 μl cell suspension was added to the upper chamber, followed by culture for 48 h (37˚C, 5% CO_2). The Transwell chamber was cleaned with PBS, fixed with 4% paraformaldehyde for 15 min at room temperature and stained with 0.1% crystal violet for 15 min at room temperature.

Tumor formation in nude mice. A total of 30 male nude mice (BALB-/c-nu, specific pathogen-free; Beijing Hufukang Biotechnology Co., Ltd.) aged 4-6 weeks (16-18 g) were randomly divided into three groups, termed PANC-1, $KRAS^{WT}$ and $KRAS^{G12D}$ and raised under the same conditions (room temperature ~26-28˚C; relative humidity ~40-60% with ventilation at ~10-15 times/h and a 10/14 h light/dark cycle). Cell suspensions of 3-5x10^6/ml were prepared in each group, a total of 100 μl of cell suspension was collected and inoculated into

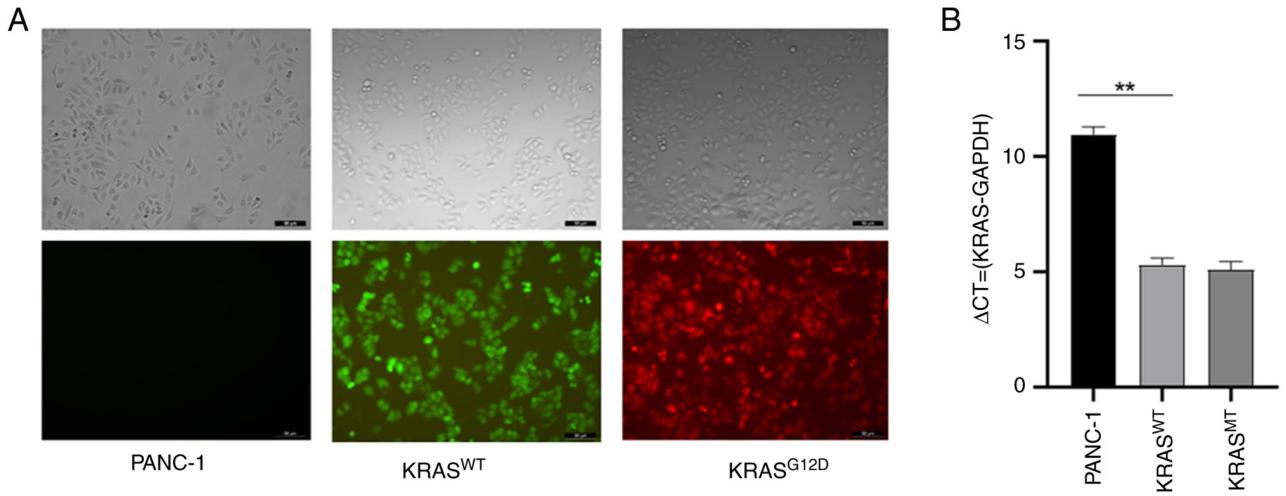

Figure 1. Efficiency of lentiviral transfection after a week of culture in medium containing 2 μg/ml purinomycin and (A) detection of infection efficiency under a microscope. (B) Reverse transcription-quantitative PCR was used to measure the expression of the KRAS gene. **P<0.01. Scale bar=50 μm. KRAS, Kirsten rat sarcoma virus; WT, wild-type.

the underarm skin of nude mice. A subcutaneous mass was observed ~1 week after inoculation, the long (a) and short diameter (b) of the tumor were measured (every other day, a total of 12 times) and the tumor volume was calculated according to the formula $ab^2/2$. Following sacrifice by cervical dislocation (mortality ascertained by the observation of respiratory, heartbeat, pupil and nervous reflex), the tumors were removed and stored in liquid nitrogen. The present study was approved by the Ethics Committee of North Sichuan Medical College (approval no. 2022035) and all procedures were carried out in accordance with relevant guidelines and regulations.

Western blotting. Cells were lysed with lysate (1 ml protein lysate mixed with 10 μl protease inhibitors) and the lysates were centrifuged at 1,3500 x g at 4˚C for 10 min. The protein concentration was detected using a BCA protein kit, according to the manufacturer's instructions. Protein lysates (30 g) were separated via 10% SDS-PAGE and transferred to PVDF membranes, which were blocked with 5% skimmed milk for 1 h at room temperature. The membranes were subsequently incubated overnight at 4˚C with the following primary antibodies: Anti-e-cadherin (1:5,000; cat. no. 60335-1; ProteinTech Group, Inc.), anti-α-E-catenin (1:3,000; cat. no. 66221-1; ProteinTech Group, Inc.), anti-MMP-9 (1:1,000; cat. no. 13667; CST), anti-MMP-3 (1:1,000; cat. no. 14351; CST), anti-STAT3 (1:1,000; cat. no. 22785, ZenBio) and anti-phosphorylated (p-) STAT3 (1:2,000; cat. no. 9145; CST). Following the primary antibody incubation, the membranes were washed three times with PBS for 15 min and incubated with HRP-conjugated goat anti-rabbit (1:5,000; cat. no. BA1039; Wuhan Boster Biological Technology, Ltd.) or anti-mouse (1:5,000; cat. no. BA1038; Wuhan Boster Biological Technology, Ltd.) secondary antibodies for 2 h at room temperature, then washed with PBS 3 times for 15 min. Protein bands were visualized with an ECL development kit (MilliporeSigma) using an enhanced chemiluminescence detection system (FUSION Fx; Vilber Lourmat).

Immunohistochemistry. Tumor tissues were fixed in 10% paraformaldehyde for >12 h at room temperature, were paraffin-embedded and sectioned (3-5 μm), and the sections were then placed into xylene for dewaxing. A descending alcohol series was added for dehydration. Sections were placed in citrate buffer (pH 6.0) for antigen retrieval (95˚C for 15 min) and the endogenous peroxidase was blocked using an endogenous peroxidase blocker (cat. no. SP-9000; OriGene Technologies, Inc.) at 25˚C for 10 min. Sections were blocked with goat serum (cat. no. SP-9000; OriGene Technologies, Inc.) at 25˚C for 10 min and then incubated with a primary antibody (α-E-catenin; 1:500; cat. no. 66221-1; ProteinTech Group, Inc.; e-cadherin; 1:2,000; cat. no. 60335-1; ProteinTech Group, Inc.; MMP-9; 1:300, cat. no. 13667; CST) for 1 h at 37˚C, washed with PBS three times and incubated with goat anti-rabbit (1:5,000; cat. no. BA1039; Wuhan Boster Biological Technology, Ltd.) or anti-mouse (1:5,000; cat. no. BA1038; Wuhan Boster Biological Technology, Ltd.) secondary antibodies at 25˚C for 15 min. Subsequently, sections were incubated with 3,3'-diaminobenzidine substrate for 5-10 min at room temperature, stained for 30 sec with hematoxylin and differentiated for 2 sec with 1% hydrochloric acid alcohol at room temperature followed by gradient alcohol series for dehydration and xylene clearing before being sealed with neutral gum and >10 fields of view were observed under a light microscope (magnification, x5; ECLIPSE 80i; Nikon Corp.).

Statistical analysis. All statistical analysis was performed by SPSS 19.0 (IBM Corp.) and GraphPad Prism 7 (GraphPad Software, Inc.) and the data are expressed as the mean ± standard deviation. One-way analysis of variance was used for multiple group comparisons and the post-hoc test was performed by the LSD method. P<0.05 was considered to indicate a statistically significant difference.

Results

$KRAS^{WT}$ gene inhibits the proliferation of continuous tumor-cell line (PANC-1). The transfection effect is shown in Fig. 1A and the verification of transfection effect was performed using RT-qPCR assay (Fig. 1B). CCK-8 and clone

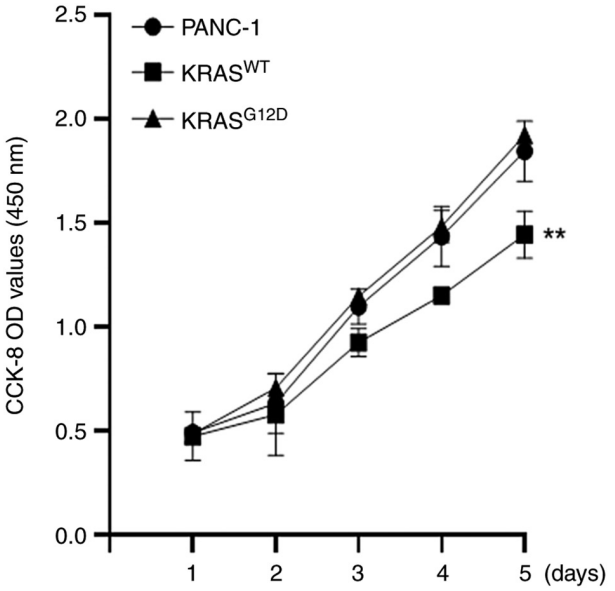

Figure 2. CCK-8 assay was used to detect cell proliferation. As compared with PANC-1 group, the proliferation of $KRAS^{WT}$ group was decreased and no statistically significant differences in the proliferation of $KRAS^{G12D}$ group were observed ($^{**}P<0.01$). KRAS, Kirsten rat sarcoma virus; WT, wild-type.

formation assays were used to detect the proliferation ability of pancreatic cancer following the overexpression of the KRAS gene. The CCK-8 assay results showed that, compared with the PANC-1, the proliferation of $KRAS^{WT}$ was reduced and the proliferation of $KRAS^{G12D}$ was not significantly changed (Fig. 2), which was consistent with the results of the colony formation assay (Fig. 3). These results indicated that the $KRAS^{WT}$ gene could inhibit the proliferation of pancreatic cancer cells.

$KRAS^{WT}$ gene inhibits the migration and invasion of PANC-1. Next, the effect of the KRAS gene on the invasion and migration of pancreatic cancer cells was investigated. Transwell and wound healing assays were performed to detect cell invasion and migration capacity. As shown in Fig. 4, the migration of $KRAS^{G12D}$ cells was enhanced and that of $KRAS^{WT}$ cells was weakened, as compared with those of PANC-1 cells after 48 h and the difference was more pronounced after 120 h. Similarly, a Transwell assay revealed an enhanced invasion of $KRAS^{G12D}$ cells and decreased invasion of $KRAS^{WT}$ cells (Fig. 5). The results suggested that the $KRAS^{WT}$ gene can inhibit the migration and invasion of pancreatic cancer.

$KRAS^{WT}$ gene may inhibit the migration and invasion of PANC-1 through the Wnt/β-catenin pathway. In order to explore the mechanism through which KRAS regulates pancreatic cancer cell invasion and migration, some signaling pathway molecules that serve key roles in cell invasion and migration were examined. E-cadherin and α-E-catenin, which are key regulators of the Wnt/β-catenin pathway, as well as MMP-3, MMP-9, STAT3 and p-STAT3 were selected for western blotting. As shown in Fig. 6, compared with PANC-1, all the expressions of proteins of $KRAS^{WT}$ were upregulated and that of $KRAS^{G12D}$ was not significantly changed. These data suggested that the inhibition of migration and invasion of PANC-1 cells by the $KRAS^{WT}$ gene may be mediated by the Wnt/β-catenin pathway.

$KRAS^{WT}$ gene inhibits tumor growth in nude mice. In order to explore the different effects of KRAS on pancreatic cancer proliferation, migration and invasion *in vivo* and *in vitro*, tumor growth curves were drawn according to the average tumor volume measured at each monitoring point. The results showed that, compared with PANC-1, the average tumor volume in the $KRAS^{WT}$ was decreased, while that of $KRAS^{G12D}$ was increased, indicating that the $KRAS^{WT}$ gene can inhibit the proliferation of pancreatic cancer *in vivo*, while the mutant KRAS gene can promote the proliferation of pancreatic cancer (Fig. 7).

$KRAS^{WT}$ gene inhibits protein expression in nude mouse tumors. Immunohistochemistry was performed on tumors from nude mice and the results showed that, compared with PANC-1, the expression of E-cadherin, α-E-catenin and MMP-9 of $KRAS^{G12D}$ exhibited no significant changes. However, the expression of E-cadherin, α-E-catenin and MMP-9 in $KRAS^{WT}$ was significantly upregulated (Fig. 8), which suggested that the inhibition of the migration and invasion of PANC-1 cells by $KRAS^{WT}$ gene may be mediated by the Wnt/β-catenin pathway.

Discussion

KRAS mutations are considered to be the driving event in the development of pancreatic cancer. Studies (13,14) have shown that KRAS mutations can be detected in 90% of pancreatic ductal intraepithelial neoplasia (PANIN), 45-60% of pancreatic ductal papillary myxomas and >90% of pancreatic adenocarcinoma, with 84% of the mutations leading to the substitution of a single amino acid at the G12 site, among which G12D is the most common (42%).

The G12D mutant subtype is associated with a decreased overall survival. Windon *et al* (9) suggested that $KRAS^{WT}$ may have a survival advantage in PDAC, as patients with $KRAS^{G12D}$ exhibited a worse survival rate and shorter overall survival time following gemcitabine-based first-line chemotherapy (11.6 vs. 5.6 months, P=0.03). Ambrogio *et al* (10) suggested that $KRAS^{WT}$ can antagonize the effect of $KRAS^{G12D}$ and the loss of $KRAS^{WT}$ can accelerate cell proliferation and tumor progression through the increase of the GTPase level of $KRAS^{G12D}$. $KRAS^{WT}$ can also disrupt the inhibitory response of $KRAS^{G12D}$ to MEK. According to Mueller *et al* (15), $KRAS^{WT}$ is absent to varying degrees during tumor development and is associated with a high mRNA expression of the $KRAS^{G12D}$ gene. Mueller *et al* also performed a microdissection of 19 patients with low-grade pancreatic intraepithelial neoplasia and deep sequencing of KRAS exon 2, confirming that $KRAS^{G12D}$ significantly increases metastatic potential, which explains the high incidence of early progression and metastasis in PDAC. The above studies show that $KRAS^{WT}$ exerts different degrees of tumor suppression. Therefore, the $KRAS^{WT}$ gene was directly overexpressed in the present study to investigate the differences in biological behaviors and the mechanism of action.

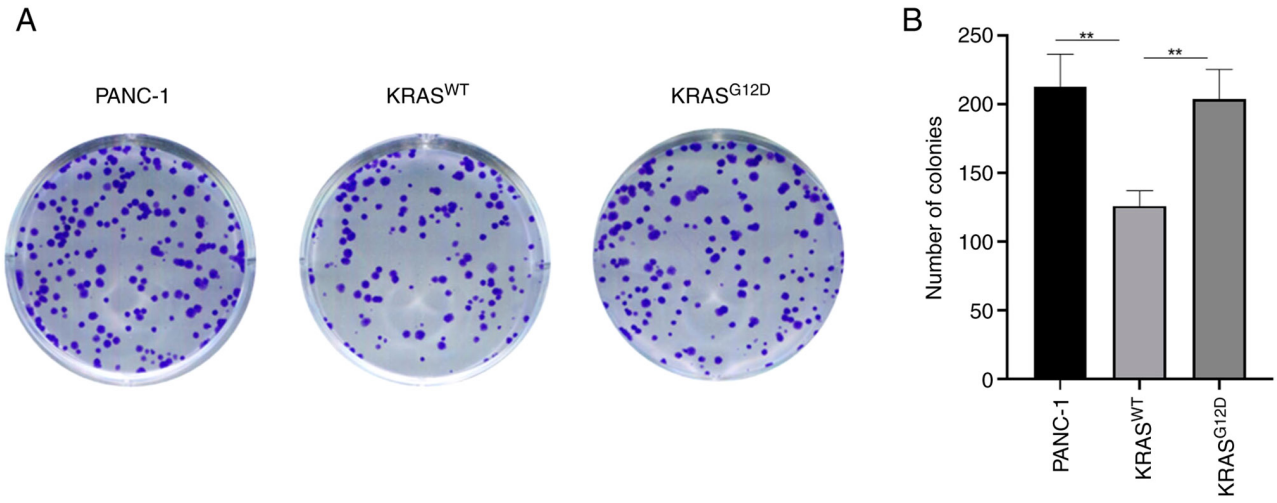

Figure 3. Colony formation assay was used to detect cell proliferation. Compared with PANC-1 group, the proliferation of $KRAS^{WT}$ group was decreased ($P<0.01$) and the changes in the proliferation of $KRAS^{G12D}$ group were not statistically significant. (A) Representative images from one of the experiments. (B) Statistical data from three experiments presented as the mean ± standard deviation ($^{**}P<0.01$). KRAS, Kirsten rat sarcoma virus; WT, wild-type.

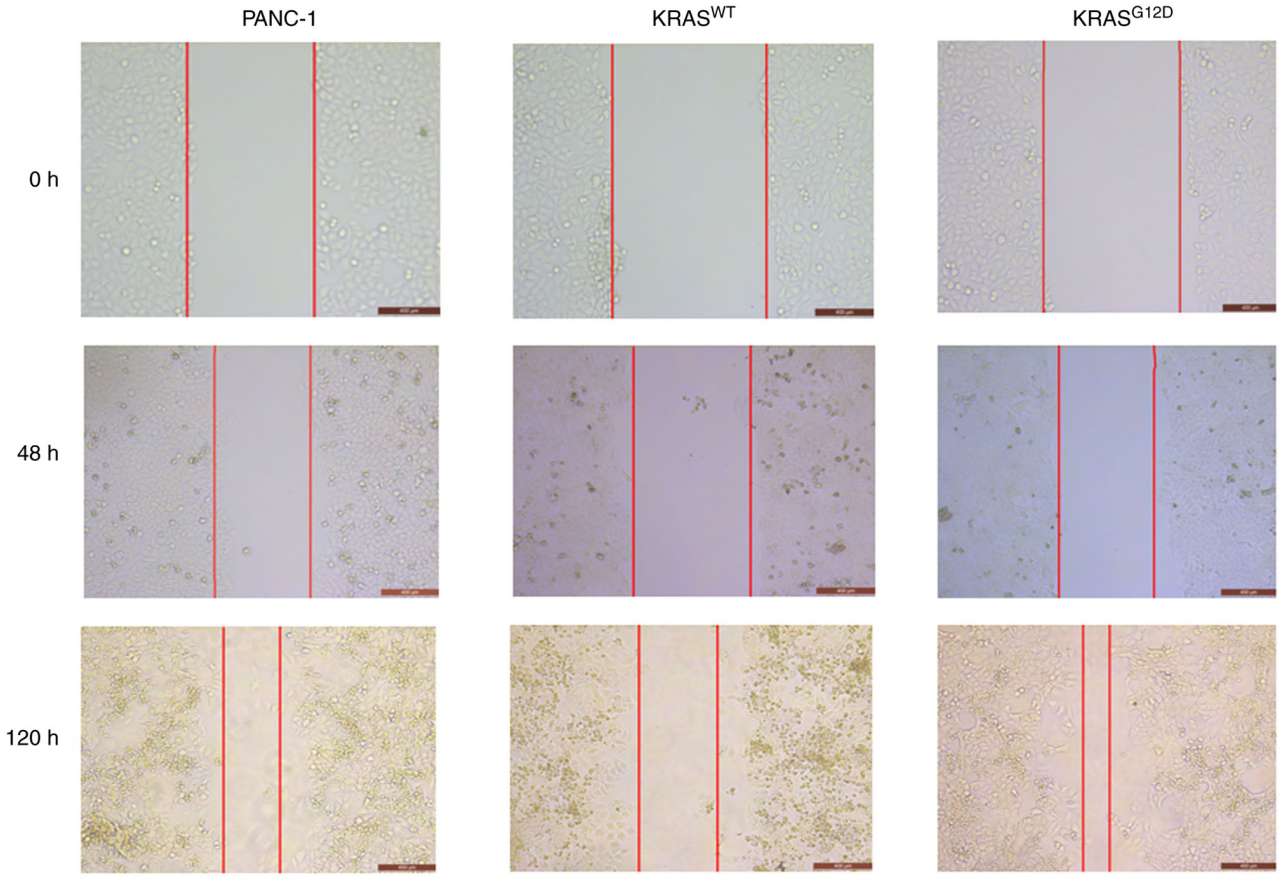

Figure 4. Wound healing assay was used to detected cell migration. As compared with PANC-1 group, the migration of $KRAS^{WT}$ group was decreased and that of $KRAS^{G12D}$ group was increased. Scale bar=400 μm. KRAS, Kirsten rat sarcoma virus; WT, wild-type.

The results of CCK-8 and clone formation assay were consistent. As compared with PANC-1, the proliferation of $KRAS^{WT}$ cells was weakened, while no significant difference was observed in $KRAS^{G12D}$, indicating that the $KRAS^{WT}$ gene can reduce the proliferation of PANC-1 (Figs. 2 and 3). At the same time, a tumor formation model of pancreatic cancer was established in nude mice (Fig. 7). *In vivo*, the average tumor volume in the $KRAS^{WT}$ group was smaller than PANC-1 group and $KRAS^{G12D}$ group, which was consistent with the results of the *in vitro* CCK-8 and clone formation assays, indicating that $KRAS^{WT}$ gene can reduce the proliferation of pancreatic cancer cells *in vivo* and *in vitro*. In addition, it was found that the tumor volume of the $KRAS^{G12D}$ group was larger than that of the PANC-1 group, indicating that the mutant KRAS gene

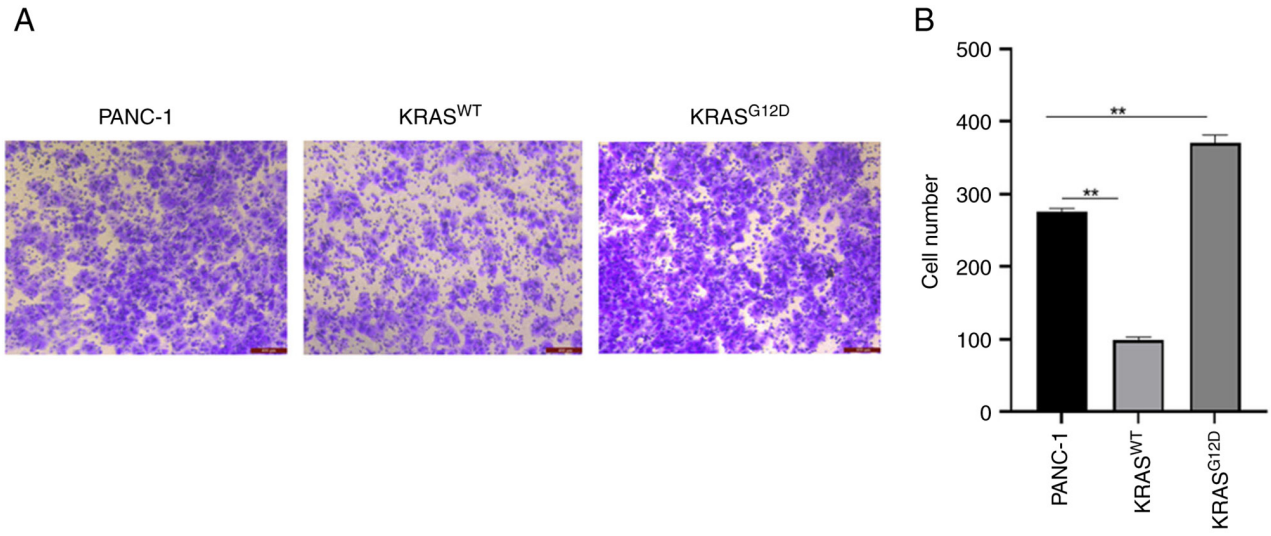

Figure 5. Transwell assay was used to detected cell invasion. Compared with PANC-1 group, the invasion of $KRAS^{WT}$ group was weakened and the invasion of $KRAS^{G12D}$ group was enhanced. (A) Representative images from one of the experiments. (B) Statistical data from three experiments presented as the mean ± standard deviation (n=3; $^{**}P<0.01$). Scale bar=400 μm. KRAS, Kirsten rat sarcoma virus; WT, wild-type.

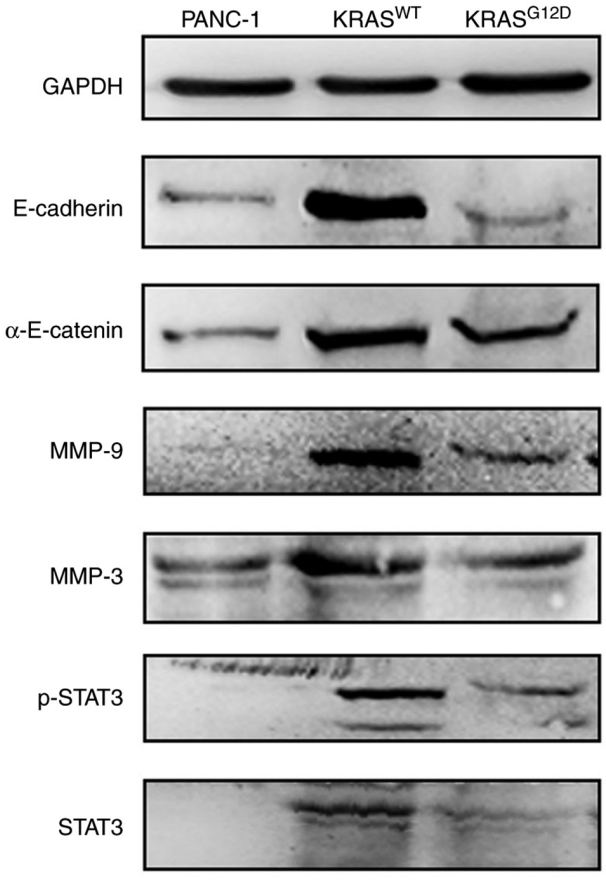

Figure 6. Protein expression detected by western blotting. As compared with PANC-1 group, the protein expression of $KRAS^{WT}$ group was increased and no significant difference was observed in $KRAS^{G12D}$ group. KRAS, Kirsten rat sarcoma virus; WT, wild-type; p-, phosphorylated.

can promote the proliferation of pancreatic cancer *in vivo*. However, the promotion effect was not obvious *in vitro*.

Wound healing and Transwell assays were then performed to detect migration and invasion. As shown in Figs. 4 and 5, as compared with PANC-1 group, the migration and invasion of $KRAS^{G12D}$ group was enhanced, while that of $KRAS^{WT}$ group was significantly weakened, suggesting that the $KRAS^{WT}$ gene could inhibit the migration and invasion of pancreatic cancer.

Epithelial-to-mesenchymal transition (EMT) is a progressive process of phenotype conversion from epithelial to mesenchymal (16,17). Among them, E-cadherin ensures the integrity of epithelial phenotypes by influencing cell polarity and tissue integrity to form stable adhesion (18), which is a key event in the EMT process (19,20). α-E-catenin also plays an important role in the regulation and coordination of intracellular adhesion and is a key regulator of the Wnt/β-catenin pathway (21). α-E-catenin is a major sensor of mechanical force in adherens junctions and its cytoplasmic domain is connected to the actin cytoskeleton by β-catenin and α-E-catenin. α-E-catenin can bind to E-cadherin to form intercellular adhesion and mediate the invasion and migration of tumor cells (22-24). E-cadherin and α-E-catenin were therefore selected to verify whether the Wnt/β-catenin pathway plays a role in inhibiting migration and invasion. According to western blotting (Fig. 6) and immunohistochemistry (Fig. 8), as compared with PANC-1, there was no significant difference in the expression of E-cadherin and α-E-catenin in $KRAS^{G12D}$. The upregulated expression of E-cadherin and α-E-catenin in $KRAS^{WT}$ indicated that the $KRAS^{WT}$ gene may play a potential role in inhibiting the invasion and migration of pancreatic cancer through the Wnt/β-catenin pathway. A previous study revealed that the expression levels of β-catenin and RAS are increased in gemcitabine-resistant pancreatic cancer cells (25); inhibition of Wnt/β-catenin and RAS/ERK pathways may provide a therapeutic strategy for gemcitabine-resistant pancreatic cancer. In fact, Wnt/β-catenin signaling and RAS/ERK pathways not only dominate gemcitabine resistance, it is possible that Wnt/β-catenin signaling directly responds to mutations in the RAS gene, which the present study confirmed.

In the process of tumor development, the destruction of basement membrane is an important step for tumor invasion and metastasis (26). In addition to degrading various protein

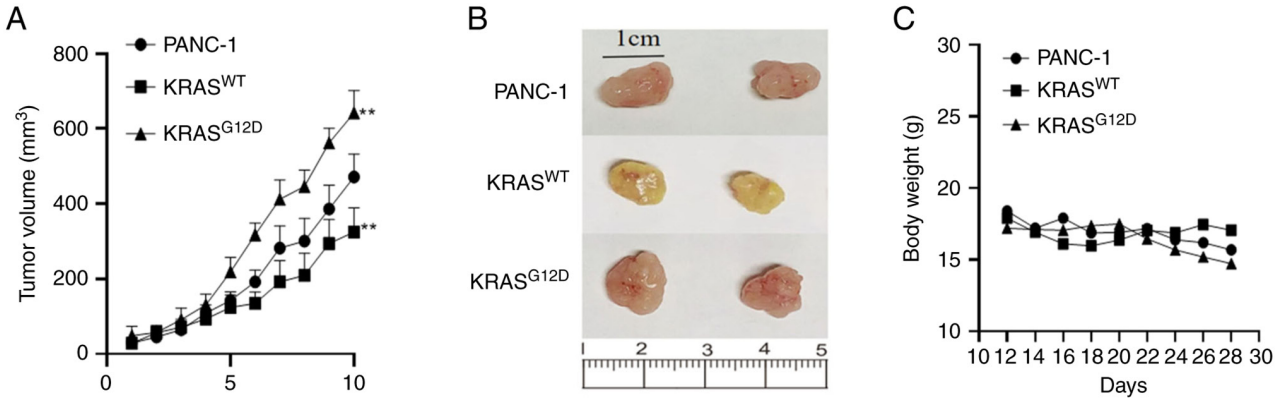

Figure 7. Tumor growth in nude mice. (A) Each group comprised 10 nude mice and the average tumor volume was calculated. Compared with PANC-1 group, the average tumor volume of $KRAS^{WT}$ group decreased and that of $KRAS^{G12D}$ group increased ($^{**}P<0.01$). (B) Images of tumors in nude mice. (C) Changes in body weight of nude mice. KRAS, Kirsten rat sarcoma virus; WT, wild-type.

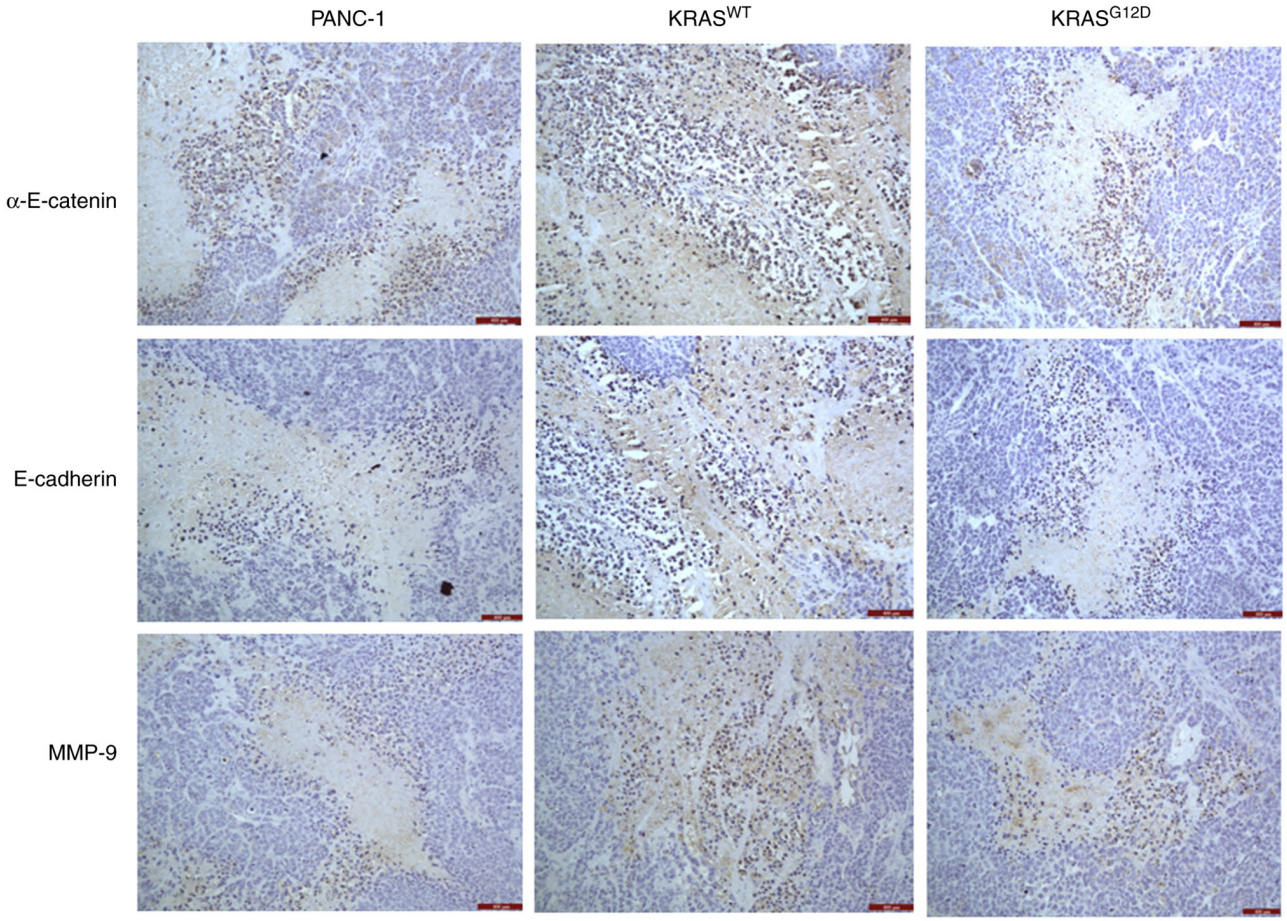

Figure 8. Immunohistochemistry was performed to detect the protein expression of tumors in nude mice. Compared with PANC-1 group, the proteins of $KRAS^{WT}$ group were all upregulated, while no significant differences were observed in $KRAS^{G12D}$ group). Scale bar=400 μm. KRAS, Kirsten rat sarcoma virus; WT, wild-type.

components of extracellular matrix, some MMPs, MMP-3, MMP-9, MMP-14 and MMP-2 can also induce EMT or its related processes (27). A previous study demonstrated that MMP-9 is highly expressed in non-small cell lung, cervical and ovarian cancer, among others, and has become one of the important factors related to cancer metastasis and invasion (28). MMP-3 protein breaks down a variety of extracellular matrix molecules and cleaves various adhesion molecules, growth factors and other MMPs (29). MMP-3 can activate MMP-1 and other family members and its overexpression is associated with the growth and metastasis of various cancers, including breast cancer (30). When stimulated by external signals, STAT3 migrates to the nucleus in the form of activated p-STAT3, which stimulates cell growth and angiogenesis, activates the transcription of target genes and

regulates cell proliferation, differentiation and metastasis (31,32). Studies have shown that STAT3/p-STAT3 is highly expressed in a variety of tumors and its activation product, p-STAT3, is associated with tumor grade and patient prognosis (33,34). As a major mediator of the JAK/STAT pathway, STAT3 may be an important regulator of tumor progression by enhancing aggressiveness or promoting EMT (35,36).

These studies indicate that the high expression of MMP-3, MMP-9, STAT3 and p-STAT3 is an important manifestation of tumor invasion and metastasis. The present results showed that, as compared with PANC-1 group, the migration and invasion of $KRAS^{WT}$ group was weakened. However, western blotting and immunohistochemistry results showed that the expression of MMP-3, MMP-9, STAT3 and p-STAT3 in $KRAS^{WT}$ group were upregulated, which was inconsistent with previous reports. The present study hypothesized that the inhibition of pancreatic cancer cell invasion and migration by the $KRAS^{WT}$ gene may not be due to the degradation of extracellular matrix or the inhibition of the function of the JAK/STAT pathway, it is also possible that the inhibitory effect of Wnt/β-catenin pathway on the invasion and migration of pancreatic cancer cells was greater compared with that of extracellular matrix or JAK/STAT pathway and the reasons need to be further studied.

In conclusion, the present study investigated the biological effects of $KRAS^{WT}$ on the proliferation and migration of pancreatic cancer cells, it was found that $KRAS^{WT}$ could inhibit the proliferation of pancreatic cancer *in vivo* and *in vitro* and mutated KRAS could enhance the proliferation of pancreatic cancer *in vivo*, but this promotion was not obvious *in vitro*. Meanwhile, $KRAS^{WT}$ can inhibit the migration and invasion of pancreatic cancer, which may be achieved through the Wnt/β-catenin pathway. The present study provided a theoretical and experimental basis for the strategy of KRAS gene therapy for pancreatic cancer.

Acknowledgements

Not applicable.

Funding

Funding was provided by the Science and Technology Innovation project of Sichuan Province (grant no. 2021033) and the Nanchong City School cooperation project (grant nos. 22SXCXTD0002 and 22SXQT0100).

Availability of data and materials

The datasets used and/or analyzed during the current study are available from the corresponding author on reasonable request.

Authors' contributions

In the planning and execution of this paper, the authors XH and CZ designed the study, XH completed the main writing and most of the experiments, CZ and RZ completed the feeding, data collection and statistical analysis of the body weight and tumor data of the nude mice., BM and JY participated in the data statistics. XH and BM confirm the authenticity of all raw data. All authors read and approved the final manuscript.

Ethics approval and consent to participate

The present study was approved by the Ethics Committee of North Sichuan Medical College (approval no. 2022035) and all procedures were carried out in accordance with relevant guidelines and regulations.

Patient consent for publication

Not applicable.

Competing interests

The authors declare that they have no competing interests.

References

1. Eguchi H, Kobayashi S, Gotoh K, Noda T and Doki Y: Characteristics of early-onset pancreatic cancer and its association with familial pancreatic cancer and hereditary pancreatic cancer syndromes. Ann Gastroenterol Surg 4: 229-233, 2020.
2. Moore A and Donahue T: Pancreatic cancer. JAMA 322: 1426, 2019.
3. Shibata H, Komura S, Yamada Y, Sankoda N, Tanaka A, Ukai T, Kabata M, Sakurai S, Kuze B, Woltjen K, *et al*: In vivo reprogramming drives Kras-induced cancer development. Nat Commun 9: 2081, 2018.
4. Luo J: KRAS mutation in pancreatic cancer. Semin Oncol 48: 10-18, 2021.
5. Moore MJ, Goldstein D, Hamm J, Figer A, Hecht JR, Gallinger S, Au HJ, Murawa P, Walde D, Wolff RA, *et al*: Erlotinib plus gemcitabine compared with gemcitabine alone in patients with advanced pancreatic cancer: A phase III trial of the National Cancer Institute of Canada Clinical Trials Group. J Clin Oncol 25: 1960-1966, 2007.
6. Drilon A, Laetsch TW, Kummar S, DuBois SG, Lassen UN, Demetri GD, Nathenson M, Doebele RC, Farago AF, Pappo AS, *et al*: Efficacy of Larotrectinib in TRK fusion-positive cancers in adults and children. N Engl J Med 378: 731-739, 2018.
7. Huang L, Guo Z, Wang F and Fu L: KRAS mutation: From undruggable to druggable in cancer. Signal Transduct Target Ther 6: 386, 2021.
8. Haigis KM: KRAS alleles: The devil is in the detail. Trends Cancer 3: 686-697, 2017.
9. Windon AL, Loaiza-Bonilla A, Jensen CE, Randall M, Morrissette JJD and Shroff SG: A KRAS wild type mutational status confers a survival advantage in pancreatic ductal adenocarcinoma. J Gastrointest Oncol 9: 1-10, 2018.
10. Ambrogio C, Kohler J, Zhou ZW, Wang H, Paranal R, Li J, Capelletti M, Caffarra C, Li S, Lv Q, *et al*: KRAS dimerization impacts MEK inhibitor sensitivity and oncogenic activity of mutant KRAS. Cell 172: 857-868 e15, 2018.
11. Kent OA: Increased mutant KRAS gene dosage drives pancreatic cancer progression: Evidence for wild-type KRAS as a tumor suppressor? Hepatobiliary Surg Nutr 7: 403-405, 2018.
12. Livak KJ and Schmittgen TD: Analysis of relative gene expression data using real-time quantitative PCR and the 2(-Delta Delta C(T)) method. Methods 25: 402-408, 2001.
13. Perets R, Greenberg O, Shentzer T, Semenisty V, Epelbaum R, Bick T, Sarji S, Ben-Izhak O, Sabo E and Hershkovitz D: Mutant KRAS circulating tumor DNA is an accurate tool for pancreatic cancer monitoring. Oncologist 23: 566-572, 2018.
14. Hobbs GA, Baker NM, Miermont AM, Thurman RD, Pierobon M, Tran TH, Anderson AO, Waters AM, Diehl JN, Papke B, *et al*: Atypical $KRAS^{G12R}$ mutant is impaired in PI3K signaling and macropinocytosis in pancreatic cancer. Cancer Discov 10: 104-123, 2020.
15. Mueller S, Engleitner T, Maresch R, Zukowska M, Lange S, Kaltenbacher T, Konukiewitz B, Öllinger R, Zwiebel M, Strong A, *et al*: Evolutionary routes and KRAS dosage define pancreatic cancer phenotypes. Nature 554: 62-68, 2018.
16. Santamaria PG, Moreno-Bueno G, Portillo F and Cano A: EMT: Present and future in clinical oncology. Mol Oncol 11: 718-738, 2017.

17. Georgakopoulos-Soares I, Chartoumpekis DV, Kyriazopoulou V and Zaravinos A: EMT factors and metabolic pathways in cancer. Front Oncol 10: 499, 2020.
18. Sommariva M and Gagliano N: E-Cadherin in pancreatic ductal adenocarcinoma: A multifaceted actor during EMT. Cells 9: 1040, 2020.
19. Loh CY, Chai JY, Tang TF, Wong WF, Sethi G, Shanmugam MK, Chong PP and Looi CY: The E-Cadherin and N-Cadherin switch in epithelial-to-mesenchymal transition: Signaling, therapeutic implications and challenges. Cells 8: 1118, 2019.
20. Christgen M, Bartels S, van Luttikhuizen JL, Bublitz J, Rieger LU, Christgen H, Stark H, Sander B, Lehmann U, Steinemann D, *et al*: E-cadherin to P-cadherin switching in lobular breast cancer with tubular elements. Mod Pathol 33: 2483-2498, 2020.
21. Wang B, Li X, Liu L, Wang M: β-Catenin: Oncogenic role and therapeutic target in cervical cancer. Biol Res 53: 33, 2020.
22. Xu XP, Pokutta S, Torres M, Swift MF, Hanein D, Volkmann N and Weis WI: Structural basis of αE-catenin-F-actin catch bond behavior. Elife 9: e60878, 2020.
23. Terekhova K, Pokutta S, Kee YS, Li J, Tajkhorshid E, Fuller G, Dunn AR and Weis WI: Binding partner- and force-promoted changes in αE-catenin conformation probed by native cysteine labeling. Sci Rep 9: 15375, 2019.
24. Rogers CD, Sorrells LK and Bronner ME: A catenin-dependent balance between N-cadherin and E-cadherin controls neuroectodermal cell fate choices. Mech Dev 152: 44-56, 2018.
25. Ryu WJ, Han G, Lee SH and Choi KY: Suppression of Wnt/β-catenin and RAS/ERK pathways provides a therapeutic strategy for gemcitabine-resistant pancreatic cancer. Biochem Biophys Res Commun 549: 40-46, 2021.
26. Kelppe J, Thoren H, Haglund C, Sorsa T and Hagstrom J: MMP-7, -8, -9, E-cadherin and beta-catenin expression in 34 ameloblastoma cases. Clin Exp Dent Res 7: 63-69, 2021.
27. Li Y, He J, Wang F, Wang X, Yang F, Zhao C, Feng C and Li T: Role of MMP-9 in epithelial-mesenchymal transition of thyroid cancer. World J Surg Oncol 18: 181, 2020.
28. Zhao Y, Qiao X, Wang L, Tan TK, Zhao H, Zhang Y, Zhang J, Rao P, Cao Q, Wang Y, *et al*: Matrix metalloproteinase 9 induces endothelial-mesenchymal transition via Notch activation in human kidney glomerular endothelial cells. BMC Cell Biol 17: 21, 2016.
29. Liutkevicius V, Lesauskaite V, Liutkeviciene R, Vaiciulis P and Uloza V: Matrix Metalloproteinases (MMP-2,-3,-9) Gene polymorphisms in cases of benign vocal fold lesions and laryngeal carcinoma. In Vivo 34: 267-274, 2020.
30. Suhaimi SA, Chan SC and Rosli R: Matrix Metallopeptidase 3 Polymorphisms: Emerging genetic markers in human breast cancer metastasis. J Breast Cancer 23: 1-9, 2020.
31. Chen XK, Gu CL, Fan JQ and Zhang XM: P-STAT3 and IL-17 in tumor tissues enhances the prognostic value of CEA and CA125 in patients with lung adenocarcinoma. Biomed Pharmacother 125: 109871, 2020.
32. Liang B, Li SY, Gong HZ, Wang LX, Lu J, Zhao YX and Gu N: Clinicopathological and prognostic roles of STAT3 and its phosphorylation in glioma. Dis Markers 2020: 8833885, 2020.
33. Song M, Wang C, Yang H, Chen Y, Feng X, Li B and Fan H: P-STAT3 inhibition activates endoplasmic reticulum stress-induced splenocyte apoptosis in chronic stress. Front Physiol 11: 680, 2020.
34. Li Y, Wang Y, Shi Z, Liu J, Zheng S, Yang J, Liu Y, Yang Y, Chang F and Yu W: Clinicopathological and prognostic role of STAT3/p-STAT3 in breast cancer patients in China: A meta-analysis. Sci Rep 9: 11243, 2019.
35. Liu HW, Lee PM, Bamodu OA, Su YK, Fong IH, Yeh CT, Chien MH, Kan IH and Lin CM: Enhanced Hsa-miR-181d/p-STAT3 and Hsa-miR-181d/p-STAT5A ratios mediate the anticancer effect of garcinol in STAT3/5A-Addicted glioblastoma. Cancers (Basel) 11: 1888, 2019.
36. Susman S, Pirlog R, Leucuta D, Mitre AO, Padurean VA, Melincovici C, Moldovan I, Crișan D and Florian SI: The role of p-Stat3 Y705 immunohistochemistry in glioblastoma prognosis. Diagn Pathol 14: 124, 2019.